

We are IntechOpen, the world's leading publisher of Open Access books Built by scientists, for scientists

6,900

Open access books available

186,000

International authors and editors

200M

Downloads

Our authors are among the

154

Countries delivered to

TOP 1%

most cited scientists

12.2%

Contributors from top 500 universities



WEB OF SCIENCE™

Selection of our books indexed in the Book Citation Index
in Web of Science™ Core Collection (BKCI)

Interested in publishing with us?
Contact book.department@intechopen.com

Numbers displayed above are based on latest data collected.
For more information visit www.intechopen.com



Antennas and Propagation for On-, Off- and In-Body Communications

Markus Grimm and Dirk Manteuffel

Additional information is available at the end of the chapter

<http://dx.doi.org/10.5772/55080>

1. Introduction

The ultra-wideband technology seems very attractive to be transferred to the challenging field of body centric communications. This technology involves the potential to establish robust communication links or high resolution localization systems. All these applications require a characterization of the propagation channel and the influence of the corresponding user to the system performance. Due to the inevitable interaction between the antenna and the related propagation channel a separation of both characteristics via traditional antenna theory methods is hardly applicable. The scope of this study is to establish a so called antenna de-embedding i.e. to separate the antenna form the underlying channel.

Traditional antenna parameters (e.g. directivity, gain, effective area) are based on free space propagation conditions. Underlying is the well known model of an isotropic radiator which enables the separation of channel, transmitter and receiver. It will be shown that this theory can be adapted to deduce approximations of equivalent antenna parameters for body centric communications. Key factor of this approach is the development of equivalent far field models of the corresponding in- and on-body scenarios. For off-body scenarios the propagation direction points away from the human body. The matching and the radiation pattern of the respective antennas may change due to the interaction with the human body but in general no modifications of the far field model are necessary. Therefore, the traditional theory is applicable with just minor restrictions and will not be discussed in further detail here.

The study is structured in two sections. The first part focuses on an in-body link i.e. the main propagation path of the electromagnetic wave leads through the tissue of the human body. Typical applications for this scenario are medical implants like wireless endoscopy or the RF breast cancer detection systems. The second part characterizes an on-body link. This means that the propagation path is defined along the body surface and the antenna is located in close proximity of the human body. The universality of this theory will be shown for the characterization of an UWB teardrop antenna.

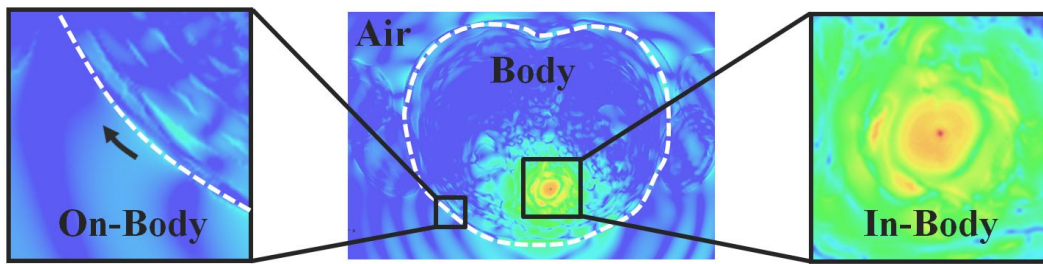


Figure 1. Distribution of the electric field of an implant located within the human abdomen; Left: On-body scenario showing surface waves guided by the body curvature; Right: In-body scenario characterized by circular shaped attenuation within the body.

2. Antenna de-embedding for in-body applications

From an electromagnetic point of view the human body consists of a large number of lossy dielectric materials of various combinations and spacial arrangements. In case of an in-body scenario the antenna is integrated into this complex dielectric structure and along an arbitrary propagation path various electromagnetic propagation effects occur. However, the most dominant effect is the attenuation of the propagating wave due to the lossy character of human tissues, see Figure 1. Furthermore, it has been shown that the average attenuation through the inhomogeneous tissue structure can be described for some scenarios by an equivalent homogeneous medium with appropriate properties [1]. In this case the analogy between the in-body and free space scenario enables an evident description of the related antenna far field. For this purpose the basic assumption of an isotropic point source is generalized for a lossy dielectric medium.

2.1. Model of an infinite homogeneous lossy dielectric media

The description of this model is based on the solution of the Helmholtz equation for a spherical wave which propagates in a homogeneous dissipative dielectric media. Due to this approach the absolute value of the electric field decreases proportionally to the reciprocal distance and shows an additional exponential attenuation with progressing distance compared to a lossless media. Therefore, the absolute value of the electric field E can be approximated by

$$E(d) \propto \frac{U_n}{d} e^{-\alpha d}, \quad (1)$$

where d , α and U_n denote the distance to the antenna, the attenuation constant of the media and a normalization factor related to the equivalent source of the spherical wave. For radiating elements, other than point sources, the accuracy of this model depends on the spacial current distribution of the source and is therefore a function of the distance. Due to the analogy of this dependency to the free space scenario the standard far field criteria seems applicable with the usual phase restrictions [2]. Related to the design of antennas which operates within the UWB frequency range [3] the radiating component is electrically large at the upper band edge frequency. In this case the appropriate far field criterium leads to following formulation:

$$d_{\text{ff}} = \frac{2D_{\text{max}}^2}{\lambda_i}, \quad (2)$$

where d_{ff} denotes the approximated far field distance, λ_1 the wave length of a TEM wave in the dielectric media at the band edge frequency and D_{max} the largest diameter of the antenna. Note that D_{max} may be increased by passively excited components in the near field of the antenna which may contribute to the radiation, like the PCB of an implant or its encapsulation. Based on this far field model it is possible to deduce the equivalent gain of an in-body antenna. Doing this it seems logically consistent to refer the normalization constant U_n to an isotropic radiator. In this case the general definition of the gain G [2] is altered to

$$G = \frac{S(d \geq d_{\text{ff}})}{S_{\text{iso,lossy}}(d \geq d_{\text{ff}})}, \quad (3)$$

where S denotes the power density of the antenna and $S_{\text{iso,lossy}}$ denotes the power density of an isotropic source in a lossy medium at the same distance. Please note, due to the fact that the propagation medium itself contains losses and the directivity is by definition a lossless quantity, the definition of the directivity is not appropriate in this case. In order to achieve a constant normalization ratio versus the distance, the losses expressed by the exponential term of equation 1 have to be taken into account. Therefore, the absolute value of the lossy isotropic power density is given by

$$S_{\text{iso,lossy}} = \frac{P_{\text{rad}}}{4\pi d^2} e^{-2\alpha d}. \quad (4)$$

In equation 4, P_{rad} denotes the radiated power of the antenna. For an antenna whose losses are restricted to the surrounding medium P_{rad} is equal to the power on the antenna P_{ant} . Due to the dissipative nature of the tissue the antenna efficiency η decreases exponentially with progressing far field distance and can be calculated by

$$\eta(d_{\text{ff}}) = \frac{1}{P_{\text{ant}}} \oint_A \mathbf{S} \cdot d\mathbf{A}, \quad (5)$$

where A is the enclosure of the antenna at the distance d_{ff} . In order to calculate the path loss between two in-body antennas, the receive properties of such antennas have to be characterized as well. Due to the fact that the equivalent tissue medium is source free, linear and isotropic the definition of the effective antenna area A_{eff} [2] is also applicable for the in-body scenario. With respect to the definition of the gain in equation 3, the effective antenna area yields

$$A_{\text{eff}} = G \frac{\lambda_1^2}{4\pi}. \quad (6)$$

Note, that the theory given above is based on an intrinsic far field model. Aim of this theory is an approach to give an intuitive formulation for the antenna design and handy path loss estimations. It raises no claim to give a closed analytical solution of the given problem. Despite this fact the model enables even estimations of theoretic problematic scenarios, such as a totally immersed antenna which is not insulated from the surrounding tissue media. As shown in [4], a theoretical formulation of this problem would lead to an inexpressible formulation. Nevertheless, to find a description between source and far field it is suggested to use an antenna which is electrically insulated from the surrounding media. Moreover the applicability of the model depends on the specific in-body scenario. The following chapter addresses the quality of the proposed model.

2.1.1. Validation of the in-body model on the example of an UWB teardrop antenna

Using the example of [1] the validity of the proposed in-body far field approach has been discussed by the evaluation of UWB localization of deep brain implants. As result it has been shown that the attenuation of an electromagnetic pulse within the inner human brain structure can be modeled by a homogeneous tissue with dielectric properties equivalent to grey matter. Despite the complex structure of the focused brain region time domain analyses indicate a radial wave conservation within the inner brain structure. These investigations indicate an average propagation velocity in arbitrary directions of the head which emphasize to the applicability of the suggested model.

The following analysis summarizes the results of an in-body scenario within the human trunk. In this case the representative media parameters are set to homogeneous muscle tissue, calculated by [5], and the validity of the approach is shown on the example of an UWB teardrop antenna. The antenna has been designed for the ultra wideband frequency range from 3.1 GHz to 10.6 GHz which is specified by [3]. Within this frequency range the return loss of the immersed teardrop antenna has been optimized to be lower than 10 dB. The capsulation of the antenna has been designed for the center frequency of 6.85 GHz by a lossless dielectric cylindrical insulation. The related permittivity of the capsulation has been set to $\epsilon_r = 49.9$ to achieve an impedance matching between the insulation and the tissue. The validation of the model has been performed by numerical calculations with the FDTD simulation software EMPIRE XCellTM [6].

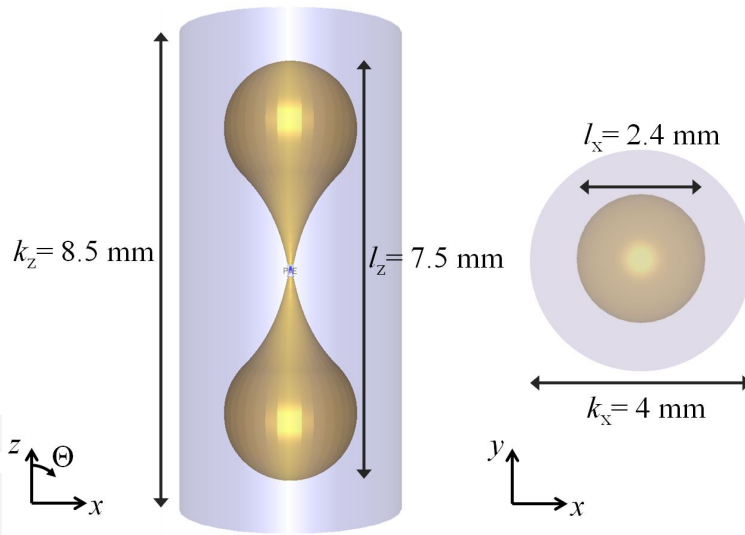


Figure 2. Insulated teardrop antenna designed for the focused UWB frequency band.

According to equation 2, the minimum far field distance for the upper band edge frequency ($f_u = 10.6$ GHz) is $d_{ff} = 3$ cm. Here, due to the insulation, the maximum antenna size D_{max} has been set to the maximal capsule dimension. The quality of the proposed far field model has been verified by the absolute difference ΔS between the calculated power density values S_{FDTD} and the far field model S_{ff} . For the angle $\Theta = 90^\circ$ the difference ΔS has been calculated at the far field distance d_{ff} by the following equation:

$$\Delta S = \frac{|S_{FDTD} - S_{ff}|}{S_{FDTD}}. \quad (7)$$

Table 1 shows the calculated values for the lower, upper and center frequency of the UWB frequency range investigated. The error rises with increasing frequency and is still within the typical range of the equivalent free space far field considerations.

	$f = 3.1 \text{ GHz}$	$f = 6.85 \text{ GHz}$	$f = 10.6 \text{ GHz}$
$\Delta S[\%]$	1.1	3.7	6.9
$G(\Theta = 90^\circ)$	1.9	2.3	3.3
$\eta_{\text{eff}}(d_{\text{ff}})$	$3.8 \cdot 10^{-2}$	$8.4 \cdot 10^{-5}$	$1.5 \cdot 10^{-8}$
$A_{\text{eff}}[m^2]$	$2.75 \cdot 10^{-5}$	$7.22 \cdot 10^{-6}$	$4.74 \cdot 10^{-6}$

Table 1. Calculated equivalent in-body antenna parameters of the UWB teardrop antenna at $d_{\text{ff}} = 3 \text{ cm}$.

Table 1 also shows the gain calculated by the equations 3 and 4. As stated, additional derivations have shown that the value is nearly constant for distances greater than d_{ff} . Nevertheless, the value is not constant within the observed frequency range and rises with increasing frequency due to the variation of the electrical length of the antenna. To characterize the losses within the near field of the antenna the efficiency has been calculated by equation 5 at the minimum far field distance d_{ff} , see Table 1. As it might be expected, the efficiency decreases drastically with increased frequency due to the higher power consumption of the tissue medium. For greater distances the efficiency decreases exponentially with increasing distance. The effective antenna area, as shown in Table 1, is calculated using equation 6. The derived values of the gain and the effective antenna area enable the approximation of the path gain for arbitrary distances greater than the minimum far field distance. This ratio of transmitted to received power (path gain) is shown for the related frequencies in Figure 3.

As shown above the model of an homogeneous dissipative medium enables the definition of antenna parameters to establish an antenna de-embedding for in-body scenarios. Therefore, the consideration of the whole system is not necessary to achieve a path loss estimation. Moreover this assumption enables a basis for a purposeful antenna development.

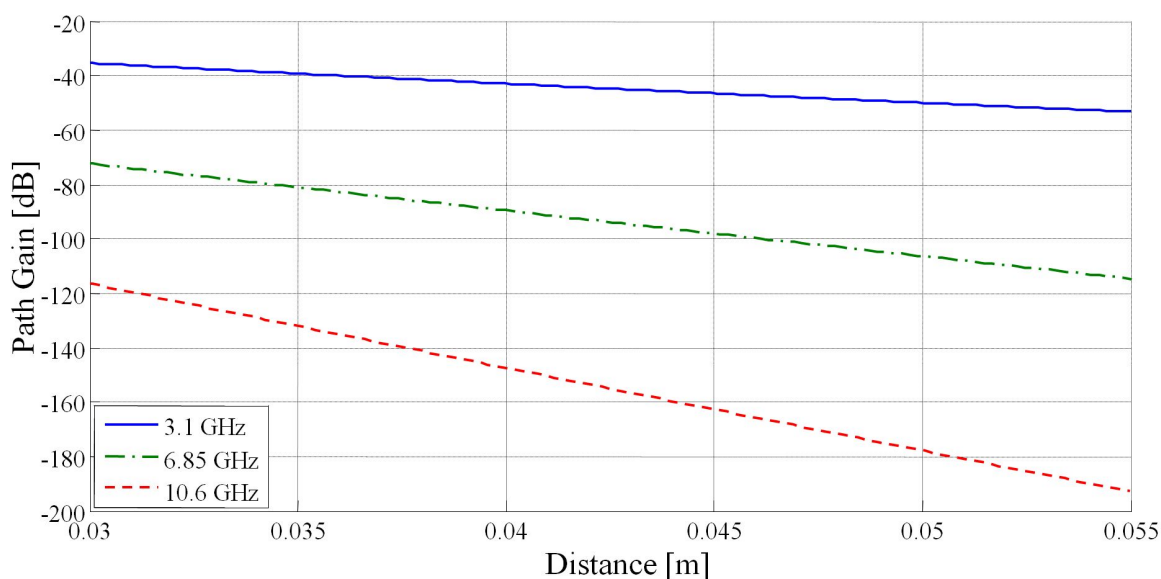


Figure 3. Calculated path gain of the UWB teardrop antenna.

2.1.2. Limitations of the in-body model

As shown in [1], boundaries between high water content tissues (muscle tissue) and air filled regions (paranasal sinus, frontal sinus) or low water content tissues (fat tissue, bone tissue) lead to various electromagnetic interactions which reduce the accuracy of the approach presented above. The average attenuation of the electromagnetic field may still be characterized by the proposed model but especially with respect to time domain analysis the multi path behavior of these structures leads to insufficient results. Moreover, the specific anatomical location of the RF application may have a strong influence on the corresponding radiation characteristic of the antenna which cannot be adequately described by a homogeneous tissue model. Despite this fact the generality of the approach enables an extension of the theory by including anatomic realistic human models in the antenna design process to derive the resulting radiation characteristic. In this case the corresponding far field distance has to be enlarged related to the anatomical structure but the average description of the far field may still be given by the proposed homogeneous model.

3. Antenna de-embedding for on-body applications

Encouraged by [7], the didactic first step to deduce a de-embedding for a wide class of on-body applications is the deduction of an adequate far field propagation model of a radiating source near a planar tissue like surface.

3.1. Model of an infinite homogeneous lossy plane surface

The propagation mechanisms of an electric doublet near a dissipative infinite homogeneous plane has been investigated in [8]. These results provide a description of the electric field components as a function of the given geometry. Therefore the absolute value of the electric field E can be calculated depending on the dipole current distribution \mathbf{i} , its effective height h , the frequency f , the complex dielectric parameters of the media ϵ and a tangential to the surface defined distance d , see Figure 4.

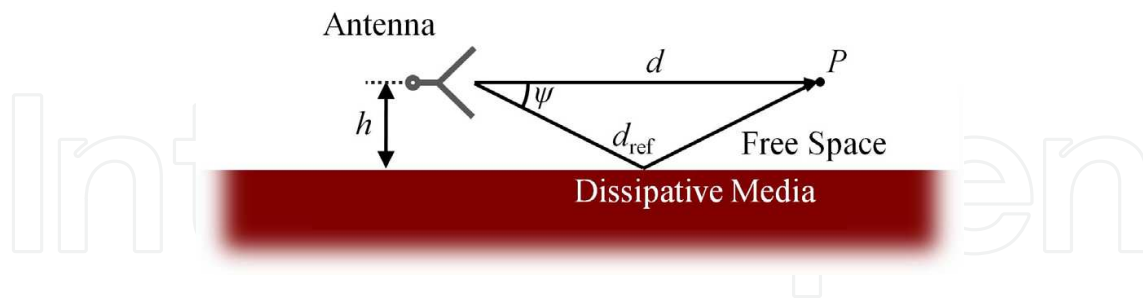


Figure 4. Principle geometry of the on-body scenario.

Included in this theory is the separation of the total electric field in its space and surface wave. As defined by Figure 4 the space wave consists of the wave components which propagates along the direct path d and the ground reflected path d_{ref} . A surface wave component which is excited by the dissipative nature of the tissue is guided by the air-media boundary. It only contributes to the related electromagnetic field if the antenna is located in close proximity to the surface. This means that the effective antenna high h is typically lower than a few wave lengths. Otherwise, this wave component is negligibly small compared to the space wave. The

electric field of any observation point P along a parallel surface path at the effective antenna high h can be described by Norton's formulation N as follows:

$$E \propto \frac{U_n}{d} N(\mathbf{i}_{v,h}, d, h, f, \underline{\epsilon}), \quad (8)$$

where the normalization value U_n depends on the antenna excitation. The term N is a function of the current distribution of the source $\mathbf{i}_{v,h}$, the distance d , the frequency f and the complex tissue permittivity $\underline{\epsilon}$. The absolute value of the electric field is given by the superposition of the space wave E_{sp} and surface wave E_{sw} as follows:

$$E(d) = E_{sp} + E_{sw}, \quad (9)$$

where E is given by

$$E(d) \propto \frac{U_n}{d} \left[\underbrace{e^{j\frac{2\pi d}{\lambda}}}_{\text{direct wave}} + \underbrace{R_{v,h} \cos^3(\psi) e^{j\frac{2\pi d_{ref}}{\lambda}}}_{\text{ground-reflected wave}} + \underbrace{(1 - R_{v,h}) F_{v,h} \cos^2(\psi) e^{j\frac{2\pi d_{ref}}{\lambda}}}_{\text{surface wave}} \right]. \quad (10)$$

In equation 10, λ denotes the free space wave length, $R_{v,h}$ the plane-wave reflection coefficient of the ground, $F_{v,h}$ the surface-wave attenuation function and d_{ref} the reflected path at angle ψ . Both, the reflection and the attenuation functions depend on the current distribution of the antenna and are given by [9] for vertical and horizontal antenna orientations. The related far field solution is valid for sufficient great distances d and depends in first place on the mathematical description of the surface-wave attenuation function. If an adequate description can be assumed the minimal valid distance, referred by Norton in [8], has to be greater than one free space wave length. An additional limitation is the assumption of locally plane waves for the derivation of the reflection coefficient of the ground. Under the assumption that the surface acts as a perfect mirror the electrical antenna size may be enlarged by the mirror image. Analog to equation 2 the far field distance d_{ff} is defined by:

$$d_{ff} = \frac{2D_{\max,eff}^2}{\lambda}, \quad (11)$$

where the modified maximum antenna dimension is denoted by $D_{\max,eff}$. For an adequate derivation of the far field distance the quantity $D_{\max,eff}$ has to be chosen appropriate under the aspect that the enlargement of the antenna by the ground acts primarily in normal direction to the surface. For distances greater than the minimum far field distance, given by equation 11, the formulation of equation 10 enables the definition of the directivity for on-body scenarios. Analog to equation 3 the directivity D is defined by the normalization of the power density to the far field model:

$$D = \frac{|S|}{|S_{Norton}|}. \quad (12)$$

The related electromagnetic field is in general a superposition of TE-, TM- and TEM-wave components and therefore a function of the parameters given in equation 8. Despite this fact, the TEM-wave component contributes the most significant part to the power flux density. Even if a strong surface wave is excited, the resulting TM-wave component is comparatively

low. This fact enables a simple approximation of the power density by the given expression of electric field:

$$D \approx \frac{|E|^2}{|E_{\text{Norton}}|^2} = \frac{|E|^2}{\left|\frac{U_n}{r} N\right|^2}. \quad (13)$$

Considering the free space and in-body definition of the directivity it is consistent to define the normalization value U_n related to a isotropic source which is modified by the function N :

$$D = \frac{|E|^2}{\frac{\eta_0 P_{\text{rad}}}{4\pi d^2} |N|^2}. \quad (14)$$

Due to the fact that the effective area of an antenna is defined for the condition in which the antenna receives a locally plane electromagnetic wave [10] the received power of an antenna inserted in the far field of the transmitting on-body antenna cannot be calculated directly by equation 6. Nevertheless, as shown by a preceding study, see [11], even for body worn antennas a derivation of the received power as a function of the incident power density is possible. The results imply a nearly constant ratio between the received power P_{out} and the incident power density S if the corresponding antennas are farther than the minimum far field distance apart. The constant ratio A'_{eff} can be calculated by

$$A'_{\text{eff}} = \frac{|P_{\text{out}}|}{|S|}. \quad (15)$$

Note, that the ratio defined by equation 15 is a function of the parameters given above and is therefore limited in its applicability to the specific setup. Apart from these aspects the equation enables the opportunity to calculate the received power as a function of arbitrary far field distances.

3.1.1. Validation of the on-body model on the example of an UWB teardrop antenna

The verification of the suggested model has been done for a vertically and horizontally orientated UWB teardrop antenna for the frequency range defined by [3]. The effective height of the antenna has been set to a quarter free space wave length at $f = 3.1$ GHz to avoid intersections between the antenna and the tissue medium. In contrast to the in-body design an encapsulation of the radiating antenna elements is not necessary to obtain an adequate matching of the antenna. The key parameters of the antenna geometry are set to $l_z = 39$ mm and $l_x = 18.5$ mm, see Figure 2, to achieve a return loss below 10 dB for the desired frequency range. The tissue properties have been set to muscle tissue, given by [5], and analog to [7] the geometry has been numerically calculated by the FDTD method presented in [6]. The minimum far field distance d_{ff} has been calculated along equation 11 and is shown in Table 2 for a vertical and horizontal orientated teardrop antenna.

Table 2 also shows the quantities D and A'_{eff} which are calculated for the minimum far field distance $d_{\text{ff,v}} = 0.54$ m and $d_{\text{ff,h}} = 0.43$ m. Analog to the in-body scenario the quality of the suggested model has been verified by the absolute difference ΔS defined by equation 7. The absolute difference shows a sufficient applicability of the suggested on-body model. In contradiction to the in-body scenario it describes a non monotone behavior for the target frequencies due to the inverse frequency dependence of the reflection coefficient of the ground and the surface-wave attenuation function defined by equation 10. As shown in Table 2, the

	$i_{v,h}$	$f = 3.1 \text{ GHz}$	$f = 6.85 \text{ GHz}$	$f = 10.6 \text{ GHz}$
$d_{ff}[\text{m}]$	v	0.16	0.35	0.54
	h	0.13	0.28	0.43
$\Delta S[\%]$	v	10.38	4.83	5.56
	h	6.64	3.15	3.48
$D[\text{lin}]$	v	1.37	1.07	0.99
	h	1.34	1.23	0.47
$A'_{\text{eff}}[\text{m}^2]$	v	$8.7 \cdot 10^{-4}$	$1.7 \cdot 10^{-4}$	$4.4 \cdot 10^{-5}$
	h	$10.3 \cdot 10^{-4}$	$1.8 \cdot 10^{-4}$	$3.4 \cdot 10^{-5}$

Table 2. Calculated on-body antenna parameters of the UWB teardrop antenna. The quantities ΔS , G and A'_{eff} are calculated for the maximum far field distance of the considered frequency range with $d_{ff,v} = 0.54 \text{ m}$ and $d_{ff,h} = 0.43 \text{ m}$.

directivity of the evaluated antennas decreases with increased frequencies. This behavior implies a reduced excitation of surface waves in the upper UWB frequency range due to the greater effective height of the antenna. Note, the derived gain is not directly comparable to the free space or in-body values. Due to the dependency of the channel model to the antenna polarization even the vertical and horizontal quantities are incomparable to each other. Despite this restriction the formulation of the directivity defines a quantity which enables an adequate discussion of various on-body antenna types and to enhance the corresponding design process.

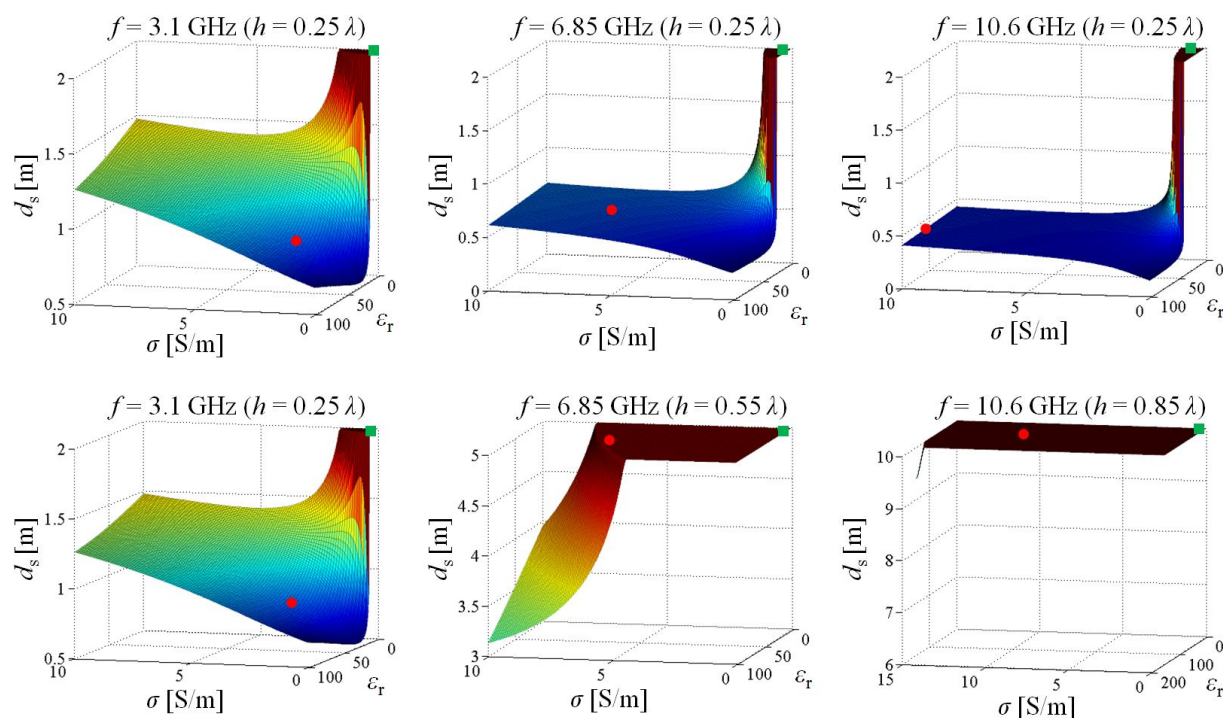


Figure 5. Distance to the antenna where the surface wave exceeds the space wave as function of the frequency and tissue parameters of a vertical polarization; First row: The effective antenna height is set to a quarter wave length of the respective frequency; Second row: Effective antenna height is set to a quarter wave length at $f = 3.1 \text{ GHz}$; Green square marker: Fat tissue; Red round marker: Muscle tissue.

Figure 5 shows an analysis of the effective antenna height in relation to the surface wave excitation. It discusses the distance d_s where the surface wave exceeds the space wave as

function of the tissue parameters. The first row shows the intersect point for effective antenna heights of a quarter wave length of the respective frequency. The second row shows the intersection point for a fixed effective antenna height which has been set to a quarter wave length of the lower UWB edge frequency ($f = 3.1$ GHz). The comparison of the results shows that with increasing frequency even at distances greater than 10 m the surface wave component is lower than the corresponding space wave. This fact implies a relatively weak far field and causes a reduction of the directivity at high frequencies. With respect to the design of future UWB on-body antennas this circumstance has to be considered. Additional investigations have also shown that vertical polarized antennas excite a much more dominant surface wave than equivalent horizontal orientated antenna configurations, see [7]. These results are in accordance to the theory given by [8] and should be considered to optimize UWB applications for given propagation scenarios.

3.1.2. Limitations of the on-body model

The validation of the suggested model with respect to the anatomical structure of the human body, with its numerous tissue types and curved surfaces, is done by a path gain calculation of a complete human body voxel model. Basis for this derivation is the numerical IT'IS virtual family Duke model [12]. The selected scenario consists of a transmitting antenna TX which is located at the right shoulder front. The corresponding receiver RX is shifted along the front side of the trunk above the right leg to the right foot. Figure 6 shows the path gain along the chosen path d . In addition, the path gain of the suggested on-body model has been calculated for homogeneous muscle and fat tissues. As seen in Figure 6, the calculated path gain of the voxel model lies between the graphs of the theoretical models.

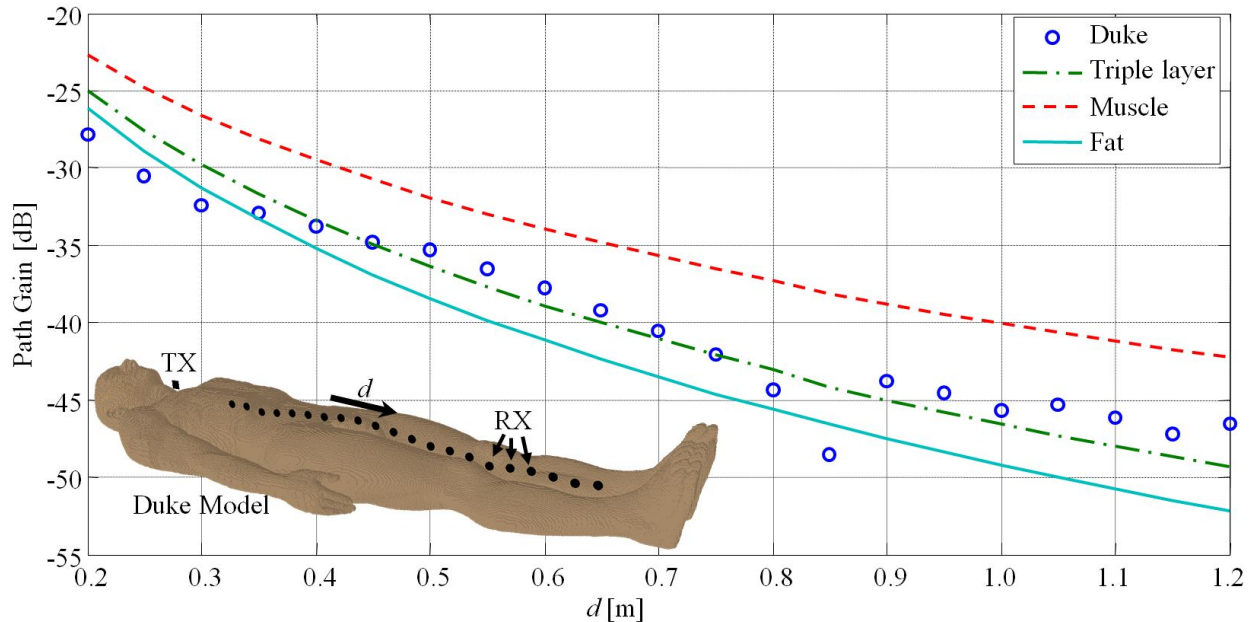


Figure 6. Path gain of the Duke voxel model in comparison to the homogeneous model of fat and muscle; Additional included is a numerical validation graph of a layered model analog to [7].

Analog to [7] a numerical model of a layered plane surface has been implemented to realize a more realistic representation of the human tissue structure. The suggested simulation model consists of 2 mm skin and 5 mm fat tissues which are positioned on an infinite muscle tissue.

As shown in Figure 6 the modified model is capable to give an adequate description of the detailed voxel simulation. In future approaches this fact can be used to enhance the presented on-body far field model by a modification of the surface-wave attenuation function $F_{v,h}$, see equation 10, by an adaption of the numeric distance as function of the surface impedance [13].

An additional effect, which is not included in the model presented, is the propagation in shadowed regions of the human body. While locally small shadowed regions are still covered by the model, large shadowed regions seem not to be described by this theory [7]. Nevertheless, these aspects have also been discussed in the last century with respects to the wave propagation above a spherical earth [9] and may also be transferred to the field of body centric communications.

4. Conclusion

The study has shown that an antenna de-embedding for in- and on-body applications can be realized by the derivation of corresponding far field models with reasonable accuracy for practical applications. Related to this theory, quantities as the directivity and the effective antenna area have been defined to derive good approximations of propagation models. Especially for on-body applications the suggested model gives a detailed insight by the separation of the electromagnetic field in its space and surface wave components.

Moreover, the presented theory enables the calculation of average path gain models of arbitrary antennas which can be reduced to a source of vertical and horizontal orientated current distributions. By this, the numerical calculation space can be reduced to the minimum far field distance of the corresponding model. Additionally, an insulated UWB tear drop antenna design has been presented for in-body communication applications to give an adequate validation example. For the on-body scenario the UWB teardrop antenna has been modified and also been discussed.

In future studies the in-body approach has to be modified to a multipath channel model to include additional propagation effects like surface waves. In addition, the on-body model has to be extended to give a wider applicability with respects to the complex structure of the human body. Moreover, the effective antenna area for on-body applications has to be described as function of the given model. With these improvements a structured combination of the on-, off- and in-body scenarios seems realizable to develop an optimized antenna theory for body centric communications.

Author details

Markus Grimm and Dirk Manteuffel
University of Kiel, Germany

5. References

- [1] Grimm, M. & Manteuffel, D. (2011). Characterization of electromagnetic propagation effects in the human head and its application to Deep Brain Implants, *IEEE-APS Topical Conference on Antennas and Propagation in Wireless Communications (APWC)*, pp. 674-677, ISBN 978-1-4577-0046-0
- [2] Balanis, C. A. (2005). *Antenna Theory*, John Wiley & Sons., ISBN 978-0-4716-6782-X

- [3] Federal Communication Commission (2002). Revision of Part 15 of the communication's rules regarding ultra wideband transmission systems. First report and order, ET Docket 98-153, FCC 02-48
- [4] Tai, C. T. & Collin, R. E. (2000). Radiation of a Hertzian Dipole Immersed in a Dissipative Medium, *IEEE Transactions on antennas and propagations*, Vol. 48, No. 10, pp. 1501-1506
- [5] Gabriel, C. & Gabriel, S. et al. (2012). An Internet Resource for the Calculation of the Dielectric Properties of Body Tissues, Italian National Research Council website, Available from: <http://niremf.ifac.cnr.it/docs/DIELECTRIC/home.html>
- [6] IMST (2012). EMPIRE XCcelTM, URL: <http://www.empire.de>
- [7] Grimm, M. & Manteuffel, D. (2010). Electromagnetic Wave Propagation on Human Trunk Models excited by Half-Wavelength Dipoles, *Antennas and Propagation Conference (LAPC)*, pp. 493-496, ISBN 978-1-4244-7304-5
- [8] Norton, K. A. (1937). The Propagation of Radio Waves over the Surface of the Earth and in the Upper Atmosphere, *Proceedings of the Institute of Radio Engineers*, , Vol. 24, No. 10, pp. 1367-1387
- [9] Norton, K. A. (1941). The Calculation of Ground-Wave Field Intensity over a Finitely Conducting Spherical Earth, *Proceedings of the Institute of Radio Engineers*, Vol. 29, No. 12, pp. 623-639
- [10] Friis, H. (1946). A Note on a Simple Transmission Formula, *Proceedings of the IRE*, Vol. 34, pp. 254-256
- [11] Grimm, M. & Manteuffel, D. (2012). Evaluation of the Norton Equations for the Development of Body-Centric Propagation Models, *European Conference on Antennas and Propagations (EUCAP)*
- [12] IT'IS Foundation (2012). Whole-Body Human Models, Enhanced Anatomical Models, URL: <http://www.itis.ethz.ch>
- [13] Wait, J.R. (1996). *Electromagnetic Waves in Stratified Media*, IEEE Press, ISBN 0-7803-1124-8